Tumor Detection of ^{18}F-PSMA-1007 in the Prostate Gland in Patients with Prostate Cancer Using Prostatectomy Specimens as Reference Method

Elin Trägårdh[1,2], Athanasios Simoulis[3], Anders Bjartell[4], and Jonas Jögi[1,2]

[1]Clinical Physiology and Nuclear Medicine, Skåne University Hospital and Lund University, Malmö, Sweden; [2]Wallenberg Centre for Molecular Medicine, Lund University, Lund, Sweden; [3]Department of Pathology, Skåne University Hospital and Lund University, Malmö, Sweden; and [4]Department of Urology, Skåne University Hospital and Lund University, Lund, Sweden

Prostate-specific membrane antigen (PSMA) radiopharmaceuticals used with PET/CT are a promising tool for managing patients with prostate cancer. This study aimed to determine the accuracy of ^{18}F-PSMA-1007 PET/CT for detecting tumors in the prostate gland using radical prostatectomy specimens as a reference method and to determine whether a correlation exists between ^{18}F-PSMA-1007 uptake and the International Society of Urological Pathology grade and prostate specific antigen (PSA) level at diagnosis. **Methods:** Thirty-nine patients referred for ^{18}F-PSMA-1007 PET/CT for initial staging and who underwent radical prostatectomy within 4 mo were retrospectively included. Uptake of ^{18}F-PSMA-1007 indicative of cancer was assessed, and SUV_{max} and total lesion uptake were calculated for the index tumor. Histopathology was assessed from radical prostatectomy specimens. True-positive, false-negative, and false-positive lesions were calculated. **Results:** In 94.9% of patients, the index tumor was correctly identified with PET. SUV_{max} was significantly higher in the tumors than in the normal prostate tissue, but no significant differences were found between different International Society of Urological Pathology grades and SUV_{max}. There was a poor correlation between PSA at diagnosis and SUV_{max} ($r = 0.23$) and moderate agreement between PSA at diagnosis and total lesion uptake ($r = 0.67$). When all tumors (also nonindex tumors) were considered, many small tumors (~1–2 mm) were not detected with PET. **Conclusion:** ^{18}F-PSMA-1007 PET/CT performs well in correctly identifying the index tumor in patients with intermediate- to high-risk prostate cancer. Approximately 5% of the index tumors were missed by PET, a finding that agrees with previous studies.

Key Words: PET/CT; PSMA; prostate; histopathology; Gleason score

J Nucl Med 2021; 62:1735–1740
DOI: 10.2967/jnumed.121.261993

Prostate cancer remains one of the most common malignancies affecting men worldwide (*1*,*2*). The correct staging of this disease is important for treatment planning and prognostication. PET/CT is recommended for detecting sites of disease recurrence in patients with prostate cancer; this recommendation has particularly been the case since the introduction of prostate-specific membrane antigen (PSMA) ligands (*3*). PET/CT using PSMA-targeting radiopharmaceuticals could potentially be suitable for initial staging because its sensitivity and specificity for detecting lymph node metastases is higher than that of conventional imaging modalities (*4*–*6*).

PSMA is a transmembrane protein often overexpressed in prostate cancer cells (*7*). It is also expressed in some other malignancies and benign tissues (*8*). Some studies indicate that PSMA expression is increased in more aggressive tumors and in castration-resistant prostate cancer (*9*–*11*). However, approximately 5%–10% of prostate cancer cells do not overexpress PSMA (*12*). PSMA ligands have been designed for radiolabeling with several radionuclides; ^{68}Ga is the most clinically common. ^{18}F-labeled PSMA agents offer advantages over ^{68}Ga-labeled ones with respect to image resolution and production amount. One promising ^{18}F-labeled PSMA radiotracer is ^{18}F-PSMA-1007 (*13*). Unlike ^{68}Ga-labeled radiopharmaceuticals, ^{18}F-PSMA-1007 is eliminated primarily via the hepatobiliary excretion route; therefore, there is almost no bladder activity, providing improved conditions for evaluation of the prostatic bed. Because only a few studies have examined ^{18}F-PSMA-1007 PET/CT as a primary T-staging modality (*14*,*15*), further studies are warranted. Kuten et al. (*15*) recently showed in a small study of intermediate- to high-risk prostate cancer patients that both ^{18}F-PSMA-1007 and ^{68}Ga-PSMA-11 could identify dominant prostatic malignancies. In their study, ^{18}F-PSMA-1007 also detected some additional low-grade lesions.

This study tested the accuracy of ^{18}F-PSMA-1007 PET/CT for detecting cancer in the prostate gland using radical prostatectomy specimens as the reference method. We then determined whether there was a correlation between the uptake of ^{18}F-PSMA-1007 and the International Society of Urological Pathology (ISUP) grade and prostate-specific antigen (PSA) level at diagnosis.

MATERIALS AND METHODS

Patients

From September 2019 to July 2020, 700 patients with biochemical recurrence after curative treatment or with newly diagnosed intermediate- or high-risk prostate cancer were examined by ^{18}F-PSMA-1007 PET/CT at Skåne University Hospital in Malmö or Lund and retrospectively included. In this cohort, 42 patients underwent radical prostatectomy for localized disease. One patient was excluded because of a long period between the PET/CT and the surgery; 2 others were excluded because of previous brachytherapy, leaving 39 patients—all were admitted for initial staging and with a time from PET/CT to surgery not exceeding 4 mo for the final analyses. This study was approved by the Regional Ethical Review Board at Lund University (approvals

Received Jan. 21, 2021; revision accepted Mar. 18, 2021.
For correspondence or reprints, contact Elin Trägårdh (elin.tragardh@med.lu.se).
Published online March 31, 2021.

2016/417 and 2018/753) and was performed in accordance with the Declaration of Helsinki. All patients gave written informed consent.

PET/CT

Four Discovery MI (GE Healthcare) PET/CT systems were used for image acquisition. Imaging was performed 120 min after radiotracer administration. The patients were scanned from the mid thigh to the base of the skull. The mean (±SD) administered ^{18}F-PSMA-1007 activity was 4.0 ± 0.4 MBq/kg (range, 3.7–6.7 MBq/kg), and the mean accumulation time was 120 ± 6 min (range, 115–153 min). The PET images were reconstructed using Q.Clear (GE Healthcare), including time-of-flight and point spread function modeling, with a 256 × 256 matrix (pixel size, 2.7 × 2.7 mm; slice thickness, 2.8 mm). Images were acquired for 2–4 min/bed position (4 min/bed position when the protocol was set up); this speed was later optimized to 2 min/bed position (*15*). The regularization factor, β, in the Q.Clear reconstruction algorithm was 500 when images were acquired at 4 min/bed position (2 patients), 600 when images were acquired at 3 min/bed position (12 patients), and 800 when images were acquired at 2 min/bed position (25 patients). The β-values for the different acquisition times were chosen to obtain a similar noise level in the images (*16*).

CT images were acquired for attenuation correction of the PET images and anatomic correlation. Diagnostic CT with intravenous and oral contrast material was performed. The tube current modulation was applied by adjusting the tube current for each individual with a noise index of 37.5 and a tube voltage of 100 kV. The slice thickness was 0.625 mm. The CT scan used for attenuation correction was acquired in the late venous phase. An adaptive statistical iterative reconstruction technique was applied.

Image Analysis

All PET/CT images were subjected to image analysis with commercially available Hermes software (Hermes Medical Solutions) by 1 experienced nuclear medicine physician. Only the patient's age and indication for the examination were known to the physician when analyzing the images. Suspected tumors in the prostate gland were characterized by SUV_{max}, tumor volume, and tumor lesion uptake (TLU) calculated as SUV_{mean} × tumor volume. These metrics were calculated by placing an automatically drawn volume of interest with a fixed threshold of 41% of tumor SUV_{max} around the suspected tumor. For some lesions with a relatively low SUV, the automatically drawn volume of interest failed, and a manual volume of interest was then drawn instead. The nuclear medicine physician marked the lesion regarded as the index lesion.

Histopathology

A second evaluation was performed by one of the authors in addition to the routine clinical evaluation of prostatectomy specimens. All slides from the radical prostatectomy specimens were annotated and evaluated using the digital pathology system Sectra Digital Pathology solution (Sectra Medical). Every tumor focus was annotated with the Gleason score, ISUP grade, and tumor localization. The index tumor was defined as the area where the tumor showed its largest dimension (*17*). No major differences between the initial reported diagnosis of Gleason score and the review were found.

Statistical Analysis

Patient demographics were analyzed descriptively. For analysis of tumor localization, each prostate was divided into 3 axial levels (base, mid, and apex) and divided at each level into 8 segments (ventral, dorsal, peripheral left and right, and central left and right) (*18*). For PET/CT and histopathology, the data for each patient were reported on a printout of the 24-segment scheme, with the tumors being marked by the nuclear medicine physician and the pathologist in a masked fashion (not being aware of the marking of the other modality). The PET/CT scan was considered to agree with the histopathology findings if the same segment was marked or if there was a discrepancy by up to 1 segment in any direction. True-positive, false-positive, and false-negative lesions were calculated. Since many of the patients had multifocal tumors, the analyses were performed both for only the index tumor and for all tumors. Associations between the ISUP grade and SUV_{max} of the index tumor were evaluated using the Kruskal–Wallis test, with a Mann–Whitney *U* test as the post hoc test. Bonferroni adjustment for multiple comparisons was applied, and adjusted *P* values are shown here. Correlations between PSA at diagnosis and SUV_{max} and TLU in the index tumor were analyzed with Spearman correlation. A *P* value of less than 0.05 was considered statistically significant. Statistical analyses were performed using SPSS, version 25 (IBM Corp.).

RESULTS

Patients

All 39 patients underwent PET/CT for initial staging. The patient characteristics are shown in Table 1. Four of the patients were on medication related to benign prostate hyperplasia (1 on a α-blocker and 3 on hormonal therapy), but no other prostate-related medication was used.

Uptake of PET Tracer in Index Tumors

An index tumor was identified in radical prostatectomy specimens in all 41 patients. The ISUP grade varied between 2 and 5, with 5 being the most common (Table 1). In 37 of 39 patients (94.9%), the same lesion was also found by PET. In all of these cases, the nuclear medicine physician had marked the lesion as index lesion. Only in 2 patients (5.4%) was the index tumor not detected by PET (not marked as a suspected tumor by the nuclear medicine physician). The median SUV_{max} was 20.1 (range, 3.7–61.7) in the index tumor and 3.7 (range, 2.4–12.4) in surrounding prostate tissue (without a pathology-proven tumor). The SUV_{max} in the surrounding prostate tissue in the 2 patients with index tumors not detected by PET was 8.3 (second highest among all patients) and 3.9, respectively. The median TLU in the index tumor was 13.6 (range, 1.5–191.8) (Table 2). The ISUP grade was 3 and 4 in the 2 patients in whom PET did not detect the index tumor; the tumors measured 35 × 19 mm and 7 × 9 mm, respectively.

A comparison between different ISUP grades and SUV_{max} for all index tumors and adjacent normal prostate tissue is shown in Figure 1. There was an overall statistically significant difference ($P < 0.0001$, Kruskal–Wallis test). The post hoc analysis showed a significant difference between normal prostate tissue and ISUP grade 2 ($P = 0.026$), ISUP grade 3 ($P = 0.001$), ISUP grade 4 ($P = 0.001$), and ISUP grade 5 ($P < 0.001$); no other comparisons were statistically significant. No statistically significant differences were found when analyzing only the different ISUP grades regarding SUV_{max} or TLU ($P = 0.18$ and $P = 0.31$, respectively; Kruskal–Wallis test). The correlation between PSA at diagnosis and SUV_{max} in the index tumor was poor ($r = 0.23$, $P = 0.17$), and that between PSA at diagnosis and TLU in the index tumor was moderate ($r = 0.67$, $P < 0.0001$) (Fig. 2)

Figure 3 shows 1 patient for whom the PET and histopathology results agreed well regarding the index tumor. Figure 4 shows 1 patient for whom the tumor was detected at histopathology and was not visualized on PET. Figure 5 shows 1 patient with false-positive uptake on PET.

PET in All Lesions

In total, 118 tumors (in 39 patients) were detected by histopathology, and 62 tumors (in 39 patients) were detected by PET. Here, 55

TABLE 1
Patient Characteristics

Parameter	Data
Age	65 ± 5.6 (53–76)
Body mass index	26.9 ± 3.2 (19.3–34.4)
Days from PET to surgery	53 ± 22 (11–105)
PSA at diagnosis (*n*)	
<10	21
10–19.9	9
≥20	9
ISUP grade	
1	
At diagnosis	1
In radical prostatectomy specimens	0
2	
At diagnosis	4
In radical prostatectomy specimens	6
3	
At diagnosis	13
In radical prostatectomy specimens	10
4	
At diagnosis	11
In radical prostatectomy specimens	9
5	
At diagnosis	11
In radical prostatectomy specimens	14
Missing	
At diagnosis	1
In radical prostatectomy specimens	0
T stage	
T1	
Clinical	16
In radical prostatectomy specimens	0
T2	
Clinical	20
In radical prostatectomy specimens	20
T3	
Clinical	3
In radical prostatectomy specimens	19

Qualitative data are number; continuous data are mean ± SD and range.

of the 118 tumors (46.6%) were classified as true PET-positive whereas the remaining 63 tumors were false-negative. Among the 63 falsely PET-negative lesions, 39 (61.9%) were very small (~1–2 mm), and 2 (3.2%) were large (7 × 9 mm and 35 × 19 mm; the 2 index tumors described above). Seven of 118 lesions (5.9%) detected by PET were false-positives based on a pathology review. In these lesions, median SUV_{max} was 11.4 (range, 6.5–13.3) and TLU was 4.9 (range, 4.2–9.5), thus being slightly lower than for true-positive lesions. No aberrant findings on histopathology were seen in areas with false-positive ^{18}F-PSMA-1007 uptake.

TABLE 2
SUV_{max} and TLU for Different ISUP Grades for 37 Index Tumors also Identified by PET, and SUV_{max} for Normal Prostate Tissue for All 39 Patients

		SUV_{max}		TLU	
Grade	*n*	Median	Range	Median	Range
Normal prostate	39	3.7	2.4–12.4	—	—
ISUP 2	6	14.5	7.9–20.9	22.2	3.7–95.2
ISUP 3	9	25.2	3.7–39.7	5.6	1.5–101.9
ISUP 4	8	19.5	8.6–31.7	12.3	7.1–58.6
ISUP 5	14	33.0	7.6–61.7	38.8	2.4–191.8

DISCUSSION

In this study, we compared the uptake of ^{18}F-PSMA-1007 with the histopathologic findings for the radical prostatectomy specimen in patients with intermediate- to high-risk prostate cancer. In most patients, the index tumor was correctly identified with PET. SUV_{max} was higher in the tumors than in normal prostate tissue, but no correlations were found between ISUP grade and SUV_{max} or between ISUP grade and TLU. There was a poor correlation between PSA at diagnosis and SUV_{max} and a moderate agreement between PSA at diagnosis and the TLU of the index tumors. When all tumors were considered, many small tumors (~1 mm) were not detected with PET. Although only 39 patients were

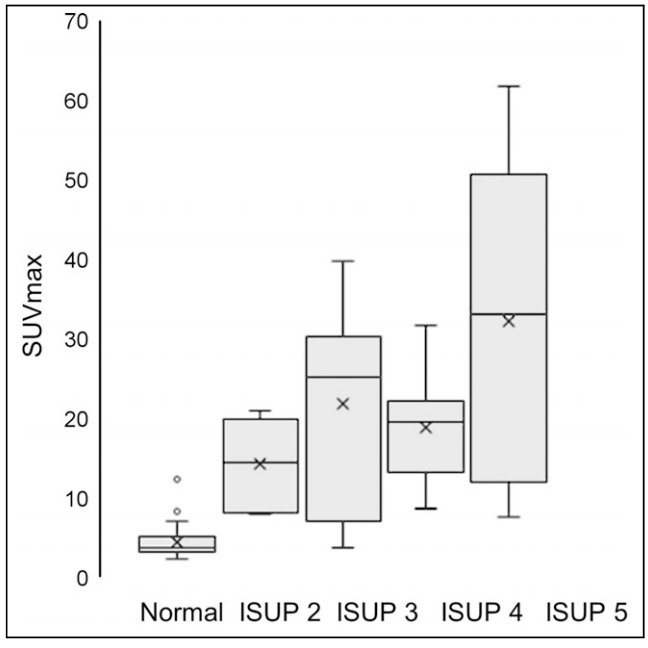

FIGURE 1. Histograms for SUV_{max} of normal prostate tissue and ISUP grades for index tumors.

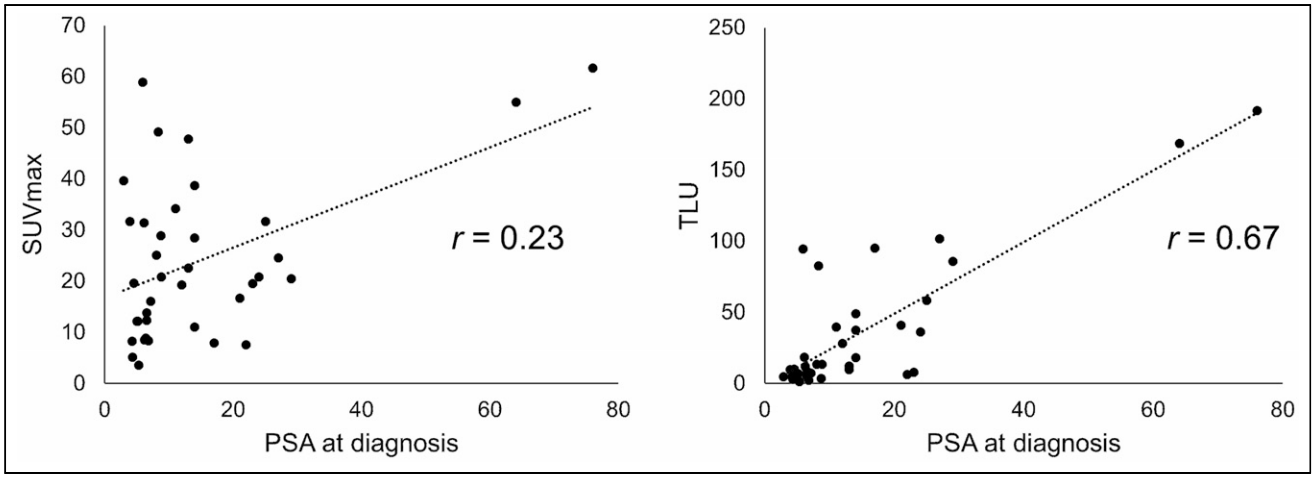

FIGURE 2. Correlation between PSA at diagnosis and SUV_{max} of index tumor (left) and between PSA at diagnosis and TLU of index tumor (right).

included, to our knowledge this was the largest study to date comparing ^{18}F-PSMA-1007 and prostatectomy specimens in patients with intermediate- to high-risk prostate cancer. Being able to correctly identify the index lesion could possibly be of interest to assist in targeted biopsies or to enable focal dose escalation during primary curative radiotherapy (*19*).

Prostate cancer cells typically show increased expression of PSMA. Benign prostatic tissue also expresses PSMA but with decreased intensity compared with prostate cancer cells. However, PSMA is not as specific as the name implies. Many conditions other than prostate cancer can overexpress PSMA (*8*). In our study, we found a small number of cases of false-positive uptake of ^{18}F-PSMA-1007. Studies have also found that not all prostate cancer cells overexpress PSMA. Maurer et al. (*4*) observed that 8% of index tumors in 130 patients with intermediate- to high-risk prostate cancer showed no or only a slight increase in ^{68}Ga-PSMA-11 uptake.

RGB

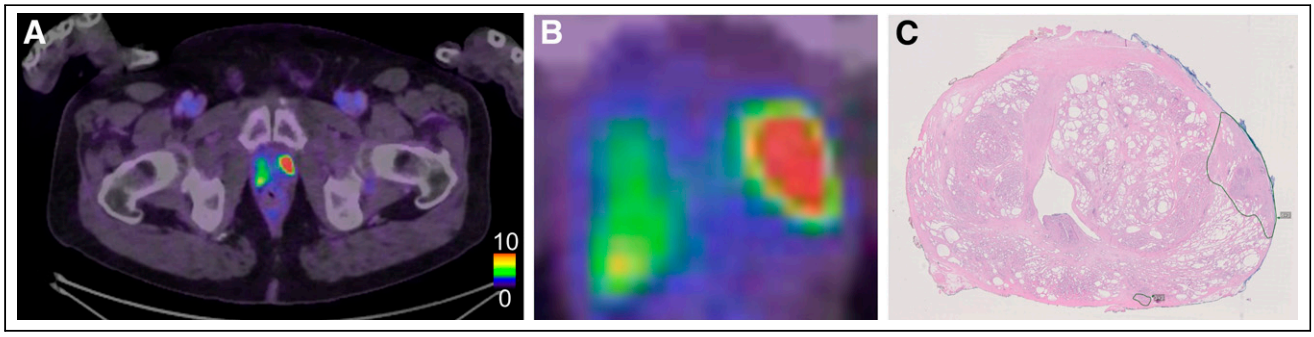

FIGURE 3. Example of 1 patient with true-positive tumor on PET. (A) PET/CT image of middle part of prostate. (B) Zoomed PET/CT image of prostate. (C) Corresponding histopathology slice delineating tumor in left part of prostate with Gleason score 4 + 3. In C, very small tumor can be seen in dorsal left part not visualized on PET. Tracer uptake in right prostate lobe is nonspecific.

RGB

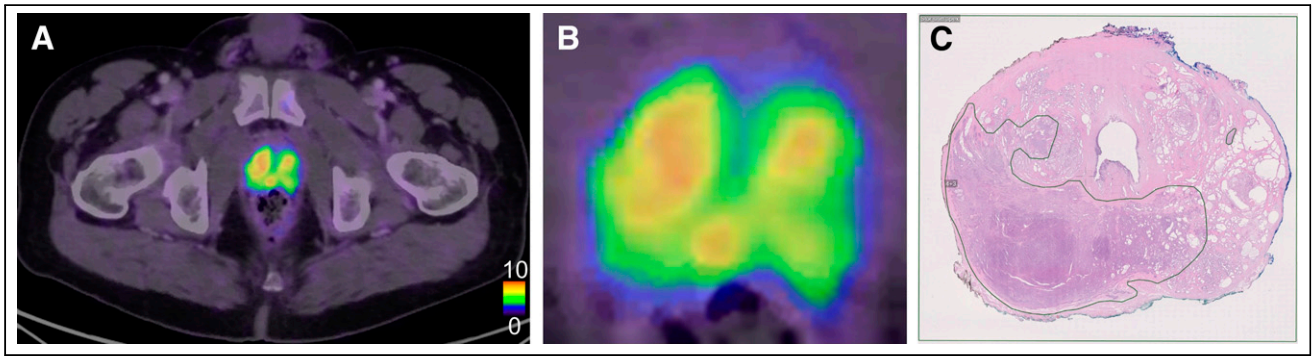

FIGURE 4. Example of 1 patient with false-negative tumor on PET. (A) PET/CT image of apical part of prostate. (B) Zoomed PET/CT image of prostate. (C) Corresponding histopathology slice delineating large tumor located mainly in dorsal right part in prostate with ISUP grade 3.

RGB

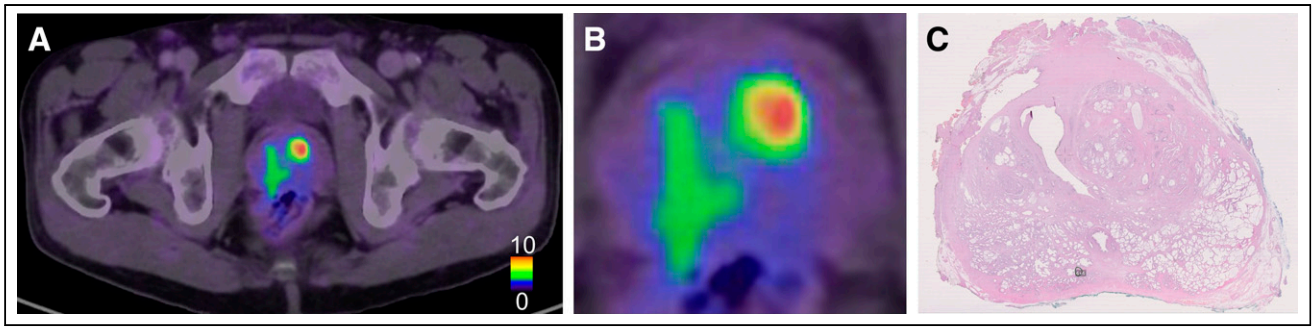

FIGURE 5. Example of 1 patient with false-positive uptake on PET in ventral left part of prostate. (A) PET/CT image of middle part of prostate. (B) Fused PET/CT image of prostate. (C) Corresponding histopathology slice without corresponding tumor. In C, we also see very small tumor in dorsal part not visualized on PET.

This finding was confirmed by Budäus et al. (*12*). In our study, only approximately 5% of the index tumors were not visualized by PET. When regarding all tumors, a considerably higher proportion of tumors was missed by PET, with most being very small tumors, which can be expected to not show up on PET because of the limited spatial resolution and partial-volume effect.

To the best of our knowledge, there was only 1 previous study comparing ^{18}F-PSMA-1007 uptake and prostatectomy specimens. Kesch et al. (*14*) studied 10 patients with biopsy-confirmed high-risk prostate patients. ^{18}F-PSMA-1007 detected the index tumor correctly in all patients but missed 2 nonindex lesions. ^{18}F-PSMA-1007 PET/CT showed 3 false-positive lesions. Similar results have been shown for a small study population using ^{68}Ga-PSMA-11 (20,21).

A previous study compared ^{68}Ga-PSMA-11 with transrectal ultrasound biopsies from 90 patients (*9*). Of these patients, 91.1% demonstrated high uptake in the index tumor that exceeded the physiologic tracer uptake in normal prostate tissue (median SUV_{max}, 12.5 vs. 3.9). In their analysis, there was a moderate correlation between PSA and SUV_{max} ($r = 0.51$) and a significantly higher SUV_{max} in tumors with a Gleason score of more than 7 than in those with a score of 3 + 3, 3 + 4, or 4 + 3. It remains unknown whether the differences from the study by Uprimny et al. regarding correlation with SUV_{max} and PSA, as well as increasing SUV_{max} with worse Gleason score or ISUP grade, can be attributed to different radiopharmaceuticals used, differences in the study population, or the lower number of patients included in our study. We found a better correlation between PSA and TLU than between PSA and SUV_{max}. TLU also considers the size of the tumor and is a better measure of tumor burden than SUV_{max}.

Some studies exist comparing multiparametric MRI and PSMA PET/CT (*22–24*). The combination has been shown to have higher sensitivity and specificity than either MRI or ^{68}Ga-PSMA-11 imaging alone for detecting intraprostatic tumors. PSMA PET could offer improved specificity whereas MRI offers improves tumor localization.

One limitation of our study was the retrospective design and the limited number of patients. Another limitation was the nature of the study cohort, with the distribution of included patients being skewed toward high risk because this is the main indication for performing PET/CT in our county. No immunostaining of PSMA expression was performed for the prostatectomy specimens. Another limitation was the challenging task of comparing PET/CT and prostatectomy specimens and difficulties in transferring both modalities into the 24-segment prostate model. Therefore, no calculations of sensitivity, specificity, and positive or negative predictive values were performed because we believe the sources of error were large and would lead to unreliable values. Finally, only 1 nuclear medicine physician and 1 pathologist made the respective evaluations.

CONCLUSION

^{18}F-PSMA-1007 PET/CT nicely identifies the index tumors in patients with intermediate- to high-risk prostate cancer, using prostatectomy specimens as the reference method. Approximately 5% of the index tumors were missed by PET, as agrees with previous findings. Small-sized nonindex tumors were often missed by PET.

DISCLOSURE

Generous financial support was provided by the Knut and Alice Wallenberg foundation, the Medical Faculty at Lund University, Region Skåne, and the Swedish Prostate Cancer Foundation. No other potential conflict of interest relevant to this article was reported.

ACKNOWLEDGMENTS

The staff of Clinical Physiology and Nuclear Medicine at Skåne University Hospital who performed the image examinations are greatly appreciated.

KEY POINTS

QUESTION: What is the accuracy of ^{18}F-PSMA-1007 PET/CT for detecting cancer in the prostate gland, using radical prostatectomy specimens as the reference method?

PERTINENT FINDINGS: In this retrospective study, we found that ^{18}F-PSMA-1007 PET/CT performs well at identifying the index tumor in patients with intermediate- to high-risk prostate cancer using prostatectomy specimens as the reference method. Small-sized nonindex tumors were often missed by PET.

IMPLICATIONS FOR PATIENT CARE: The results indicate that ^{18}F-PSMA-1007 PET/CT is a reliable method for detecting prostate cancer.

REFERENCES

1. Cornford P, Bellmunt J, Bolla M, et al. EAU-ESTRO-SIOG guidelines on prostate cancer. Part II: treatment of relapsing, metastatic, and castration-resistant prostate cancer. *Eur Urol.* 2017;71:630–642.

2. Mottet N, Bellmunt J, Bolla M, et al. EAU-ESTRO-SIOG guidelines on prostate cancer. Part 1: screening, diagnosis, and local treatment with curative intent. *Eur Urol.* 2017;71:618–629.
3. Perera M, Papa N, Christidis D, et al. Sensitivity, Specificity, and Predictors of Positive ^{68}Ga-prostate-specific membrane antigen positron emission tomography in advanced prostate cancer: a systematic review and meta-analysis. *Eur Urol.* 2016;70:926–937.
4. Maurer T, Gschwend JE, Rauscher I, et al. Diagnostic efficacy of ^{68}gallium-PSMA positron emission tomography compared to conventional imaging for lymph node staging of 130 consecutive patients with intermediate to high risk prostate cancer. *J Urol.* 2016;195:1436–1443.
5. Herlemann A, Wenter V, Kretschmer A, et al. ^{68}Ga-PSMA positron emission tomography/computed tomography provides accurate staging of lymph node regions prior to lymph node dissection in patients with prostate cancer. *Eur Urol.* 2016;70:553–557.
6. Rowe SP, Macura KJ, Mena E, et al. PSMA-based ^{18}F]DCFPyL PET/CT is superior to conventional imaging for lesion detection in patients with metastatic prostate cancer. *Mol Imaging Biol.* 2016;18:411–419.
7. Leek J, Lench N, Maraj B, et al. Prostate-specific membrane antigen: evidence for the existence of a second related human gene. *Br J Cancer.* 1995;72:583–588.
8. Sheikhbahaei S, Afshar-Oromieh A, Eiber M, et al. Pearls and pitfalls in clinical interpretation of prostate-specific membrane antigen (PSMA)-targeted PET imaging. *Eur J Nucl Med Mol Imaging.* 2017;44:2117–2136.
9. Uprimny C, Kroiss AS, Decristoforo C, et al. ^{68}Ga-PSMA-11 PET/CT in primary staging of prostate cancer: PSA and Gleason score predict the intensity of tracer accumulation in the primary tumour. *Eur J Nucl Med Mol Imaging.* 2017;44:941–949.
10. Silver DA, Pellicer I, Fair WR, Heston WD, Cordon-Cardo C. Prostate-specific membrane antigen expression in normal and malignant human tissues. *Clin Cancer Res.* 1997;3:81–85.
11. Bostwick DG, Pacelli A, Blute M, Roche P, Murphy GP. Prostate specific membrane antigen expression in prostatic intraepithelial neoplasia and adenocarcinoma: a study of 184 cases. *Cancer.* 1998;82:2256–2261.
12. Budäus L, Leyh-Bannurah SR, Salomon G, et al. Initial experience of ^{68}Ga-PSMA PET/CT imaging in high-risk prostate cancer patients prior to radical prostatectomy. *Eur Urol.* 2016;69:393–396.
13. Giesel FL, Hadaschik B, Cardinale J, et al. F-18 labelled PSMA-1007: biodistribution, radiation dosimetry and histopathological validation of tumor lesions in prostate cancer patients. *Eur J Nucl Med Mol Imaging.* 2017;44:678–688.
14. Kesch C, Vinsensia M, Radtke JP, et al. Intraindividual comparison of ^{18}F-PSMA-1007 PET/CT, multiparametric MRI, and radical prostatectomy specimens in patients with primary prostate cancer: a retrospective, proof-of-concept study. *J Nucl Med.* 2017;58:1805–1810.
15. Kuten J, Fahoum I, Savin Z, et al. Head-to-head comparison of ^{68}Ga-PSMA-11 with ^{18}F-PSMA-1007 PET/CT in staging prostate cancer using histopathology and immunohistochemical analysis as a reference standard. *J Nucl Med.* 2020;61:527–532.
16. Tragardh E, Minarik D, Brolin G, Bitzen U, Olsson B, Oddstig J. Optimization of [^{18}F]PSMA-1007 PET-CT using regularized reconstruction in patients with prostate cancer. *EJNMMI Phys.* 2020;7:31.
17. Renshaw AA, Richie JP, Loughlin KR, Jiroutek M, Chung A, D'Amico AV. Maximum diameter of prostatic carcinoma is a simple, inexpensive, and independent predictor of prostate-specific antigen failure in radical prostatectomy specimens: validation in a cohort of 434 patients. *Am J Clin Pathol.* 1999;111:641–644.
18. PI-RADS Prostate Imaging–Reporting and Data System. American College of Radiology website. https://www.acr.org/-/media/ACR/Files/RADS/PI-RADS/PIRADS-V2-1.pdf. Published 2019. Accessed August 31, 2021.
19. Kerkmeijer LGW, Groen VH, Pos FJ, et al. Focal boost to the intraprostatic tumor in external beam radiotherapy for patients with localized prostate cancer: results from the FLAME randomized phase III trial. *J Clin Oncol.* 2021;39:787–796.
20. Rhee H, Thomas P, Shepherd B, et al. Prostate specific membrane antigen positron emission tomography may improve the diagnostic accuracy of multiparametric magnetic resonance imaging in localized prostate cancer. *J Urol.* 2016;196:1261–1267.
21. Rahbar K, Weckesser M, Huss S, et al. Correlation of intraprostatic tumor extent with ^{68}Ga-PSMA distribution in patients with prostate cancer. *J Nucl Med.* 2016; 57:563–567.
22. Eiber M, Weirich G, Holzapfel K, et al. Simultaneous ^{68}Ga-PSMA HBED-CC PET/MRI improves the localization of primary prostate cancer. *Eur Urol.* 2016;70: 829–836.
23. Hicks RM, Simko JP, Westphalen AC, et al. Diagnostic accuracy of ^{68}Ga-PSMA-11 PET/MRI compared with multiparametric MRI in the detection of prostate cancer. *Radiology.* 2018;289:730–737.
24. Park SY, Zacharias C, Harrison C, et al. Gallium 68 PSMA-11 PET/MR imaging in patients with intermediate- or high-risk prostate cancer. *Radiology.* 2018;288: 495–505.